Sintering of Cu–Al$_2$O$_3$ nano-composite powders produced by a thermochemical route

MARIJA KORAĆ[1]*, ZORAN ANĐIĆ[2], MILOŠ TASIĆ[2] and ŽELJKO KAMBEROVIĆ[1]

[1]Faculty of Technology and Metallurgy, Karnegijeva 4, 11000 Belgrade and
[2]The Scientific Research Center, Nikole Pasica 26, 31000 Užice, Serbia

Abstract: This paper presents the synthesis of nano-composite Cu–Al$_2$O$_3$ powder by a thermochemical method and sintering, with a comparative analysis of the mechanical and electrical properties of the obtained solid samples. Nano-crystalline Cu–Al$_2$O$_3$ powders were produced by a thermochemical method through the following stages: spray-drying, oxidation of the precursor powder, reduction by hydrogen and homogenization. Characterization of powders included analytical electron microscopy (AEM) coupled with energy dispersive spectroscopy (EDS), differenttial thermal and thermogravimetric (DTA–TGA) analysis and X-ray diffraction (XRD) analysis. The size of the produced powders was 20–50 nm, with a noticeable presence of agglomerates. The composite powders were characterized by a homogenous distribution of Al$_2$O$_3$ in a copper matrix. The powders were cold pressed at a pressure of 500 MPa and sintered in a hydrogen atmosphere under isothermal conditions in the temperature range from 800 to 900 °C for up to 120 min. Characterization of the Cu–Al$_2$O$_3$ sintered system included determination of the density, relative volume change, electrical and mechanical properties, examination of the microstructure by SEM and focused ion beam (FIB) analysis, as well as by EDS. The obtained nano-composite, the structure of which was, with certain changes, presserved in the final structure, provided a sintered material with a homogeneous distribution of dispersoid in a copper matrix, with exceptional effects of reinforcement and an excellent combination of mechanical and electrical properties.

Keywords: copper, alumina, powder, nano-composite, sintering.

INTRODUCTION

Research of nano-crystalline materials has intensified in recent years, primarily due to their attractive potential, *i.e.*, their properties which are significantly improved compared to conventional grain materials.[1–3] Nano-structured materials rank in the group of ultra fine, metastable structures containing a high concentration of defects (point defects, dislocations) and boundaries (grain boundaries, interphase boundaries, *etc.*). These materials are structurally different from crystals and amor-

1115

phous forms because of the fact that grain boundaries and interphases represent a specific state of the solid matter, since the atoms on boundaries are subjected to a periodical potential field of the crystal from both sides of the boundary.[2] Nano-structured materials can be synthesized in controlled processes by the following methods: condensation from the gas phase, synthesis in vacuum, high energy reactive milling, solution precipitation (sol–gel, hydrothermal synthesis, electrochemical synthesis, reactions in aerosol-reactive spraying, sublimation drying).[2,4]

The introduction of fine dispersed particles into a metal matrix has significant reinforcing effects, which can be maintained at elevated temperatures. For such a reinforcement, ultra fine and nano-particles of oxides are suitable, which, due to their hardness, stability and insolubility in the base metal, also represent obstacles to dislocation motion at elevated temperatures. The maximum effects of reinforcement are achieved by an even distribution of oxide particles and short distances of their fine dispersion in the matrix of the base metal.[4] Research of dispersion reinforced materials, indicates the significance of the properties of the starting powders and the importance of the starting structure, which, although undergoing certain changes during the further processing, basically remains preserved in the structure of the final product.[3,5] A very important aspect of dispersion strengthening is also the introduction of as small as possible amount of dispersed particles into the volume of the base material.

The above characteristics significantly determine the later-stage processing and sintering properties and eventually determine the microstructure of the composite. Uniform powder shape and a narrow size distribution provide reduced microstructural defects in the sintered composites, by enhancing powder flow and packing efficiency during slip casting and cold isostatic pressing (CIP).[6]

Obtaining powders by a thermochemical method, in which the input materials are in the liquid state, is not a new procedure but recently, due to the development of contemporary materials with advanced properties, intensive interest in this method for production of ultra fine and nano-powders has occurred.[7−9] According to Jena *et al.*[8,10] the synthesis of nano-composite powders by a chemical method is possible in two ways. The first method comprises adding of a certain quantity of CuO into a solution of aluminum nitrate. In the second synthesis method, aluminum nitrate and CuO are also mixed in appropriate proportions in distilled water. However, in this case, ammonium hydroxide is added to form a gel for the hydrolysis of aluminum nitrate to hydroxide. In both cases, the mixture was annealed at 850 °C and then reduced in a hydrogen atmosphere at 975 °C for 2 h until the final structure was obtained.

Nano-powders give better performance in sintering due to their high surface area and, therefore, can tremendously improve the sintering process. The part produced with nano-powders will have a high density, hardness and fracture toughness.[11]

Sintering of ultradispersed powders occurs due to sliding of the particles along their borders,[7] followed by a dislocative mechanism responsible for the creation

of surplus vacancies. The concentration of surplus vacancies can reach a value corresponding to the concentration of vacancies in the range of temperatures near the melting temperature of the materials. On this basis, it could be concluded that diffusion activity during sintering of ultradispersed particles in the area of really low temperatures (0.1–0.3 T_m) is conditioned by the presence of unbalancing "recrystallization" vacancies. The high recrystallization rate of ultradispersed particles is the consequence of a self-activated recrystallization process.

EXPERIMENTAL

Previous papers related to a similar topic[12] show soluble nitrates of copper and aluminum, Cu(NO$_3$)$_2$·3H$_2$O and Al(NO$_3$)$_3$·9H$_2$O, could be used as a transient components for the thermochemical synthesis of nano-composite Cu–Al$_2$O$_3$ powders.

The synthesis process in this work followed four stages:

– making a 50 wt. % aqueous solution of Cu(NO$_3$)$_2$ and Al(NO$_3$)$_3$·9H$_2$O; the quantities of salts were taken so that the required composition of the Cu–Al$_2$O$_3$ nano-composite system with 3 and 5 wt. % of alumina would be attained;

– spray drying using a modified house sprayer at a temperature 180 °C to produce the precursor powder;

– annealing of precursor powder in an air atmosphere at 900 °C for 1 h, thereby forming copper oxide and the phase transformation of Al$_2$O$_3$ to the thermodynamically stable phase (α-Al$_2$O$_3$);

– reduction of thermally treated powders in a hydrogen atmosphere at a temperature of 400 °C for one hour, whereby the copper oxide was transformed into elementary copper and the α-Al$_2$O$_3$ remained unchanged;

– homogenization in a jar mill, type TMF HM1, with milling chamber dimensions of: internal diameter 180 mm, height 160 mm and volume 4 l.

Characterization of the synthesized powders included AEM (JEOL 200CX), XRD (Siemens D500 PC, CuKα, 2θ = 1–100°, step (2θ) 0.02° and DTA–TGA (Netzch STA model 49EP).

After characterization, the powders were cold pressed from the both sides in an appropriate tool, 8×32×2 mm^3 at a compacting pressure of 500 MPa. A laboratory hydraulic power press "Zim", Russia, was used for the pressing. The obtained samples were sintered in a hydrogen atomsphere under isothermal conditions at two different temperatures, 800 and 900 °C, for 30, 60, 90 and 120 min. Sintering was performed in a laboratory electroresistance tube furnace, power 3 kW with thermoregulation ±1 °C. The internal diameter of the furnace was 45 mm and the length 100 cm. The maximum temperature in working area (55 cm) was 1300±1 °C.

The characterization of the sintered system of nano-composite Cu–Al$_2$O$_3$ included determination of the density, relative volume change, electrical and mechanical properties and examination of the microstructure by SEM, as well as by EDS analysis.

RESULTS AND DISCUSSION

Characterization of the Cu–Al$_2$O$_3$ powders

DTA–TGA Analysis of the nano-composite Cu–Al$_2$O$_3$ powder with 5 wt. % Al$_2$O$_3$, obtained by the thermochemical procedure, showed two endothermic peaks, at approximately 150 and 250 °C, which are related to the evaporation and dehydration of the residual moisture. The exothermic peak at 324 °C is accompanied by a mass increase of 5.88 %, which represents the beginning of the oxidation process of the fine copper powder present. An intensive mass increase was

registered on the TG curve at a temperature of approximately 550 °C, thereafter only an insignificant mass increase of some percents occurred, whereas the overall mass increment during heating was 28.43 %. A further increase of the temperature indicated the existence of four exothermic peaks at 684, 820, 885 and 938 °C, which correspond to the phase transformations of Al_2O_3 occurring in the system.

Only peaks corresponding to the nitrates of copper and aluminum were identified in the structure during XRD examination of the precursor powder produced by spray drying an aqueous solution of copper and aluminum nitrates, which is in accordance with the experiment set-up.[13] X-Ray diffraction analysis after annealing the dried powder exhibited peaks corresponding to CuO and Al_2O_3, as well as one unidentified peak. According to Lee,[9] this peak corresponds to a third phase, $Cu_xAl_yO_z$ which appears in the structure due to the eutectic reaction of $(Cu+Cu_2O)$ with Al_2O_3. The formation of this phase is thermodynamically possible on Cu–Al contact surfaces. During eutectic joining of copper and Al_2O_3, the eutecticum formed by heating up to the eutectic temperature expands and reacts with Al_2O_3 creating $Cu_xAl_yO_z$, which is compatible with both phases on the inter-surface. XRD analysis of the powder after reduction shows the presence of peaks corresponding to elementary copper and Al_2O_3.[13]

The characterization of the nano-composite Cu–Al_2O_3 powder obtained by the thermochemical procedure also included examination by AEM, the results of which are shown in Fig. 1.

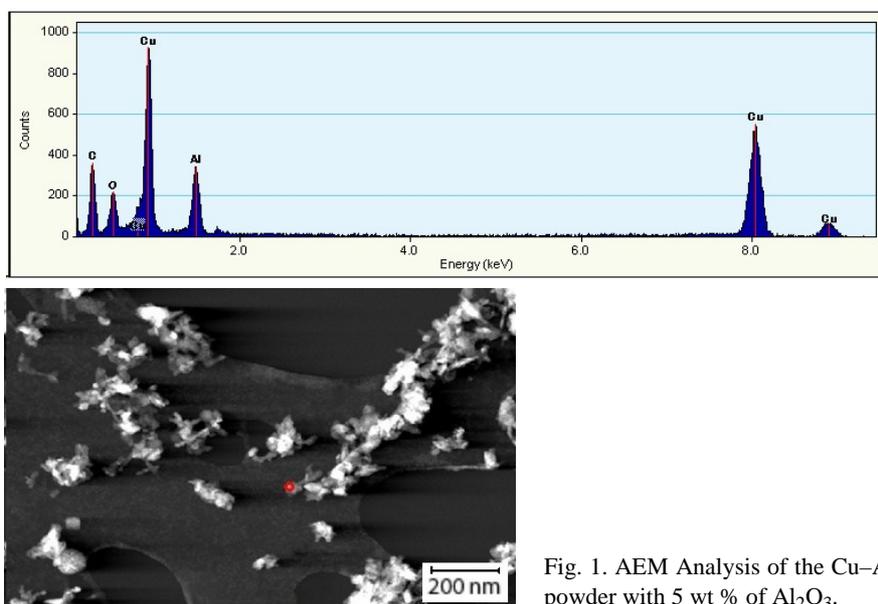Fig. 1. AEM Analysis of the Cu–Al_2O_3 powder with 5 wt % of Al_2O_3.

Typical microstructural analysis of the powders shows the possibility of synthesis of the nano-composite Cu–Al_2O_3 system by the thermochemical proce-

dure, starting from aqueous nitrate solutions. Particles with a size of 20–50 nm are clearly visible, as well as the presence of agglomerates >100 nm. The particles are irregularly shaped, with the presence of individual nodular particles with a rough surface morphology.

The agglomeration of finer particles is a consequence of their large surface, *i.e.*, high surface energy, and the effect of bonding forces between them. Due to the contacts between the particles, interatomic bonds were formed. The magnitude of those bonds depends directly on surface energy of particles. Taking into account the appearance of agglomerates, particular attention will be paid in future research to the production of non-agglomerated powders, where surface-active agents will be used for de-agglomeration. Presently, the application of poly(ethylene glycol)[14] and ultrasonification[15–17] are considered.

Sintering

The results of density examination, relative volume change, specific electric resistance and hardness are given in Table I.

TABLE I. Average density, $\Delta V/V_0$, specific electric resistance and hardness of the sintered samples of Cu–Al$_2$O$_3$ with different aluminum content

t / °C	Time min	Density g cm^{-3}	$\Delta V/V_0$ (average)	Specific electric resistance 10^{-6} Ω m	Hardness HRB 10/40 (average)
Cu + 3 wt. % Al$_2$O$_3$					
800	15	5.58	0.1042	0.07413	88.2
	30	5.62	0.1194	0.07128	94.1
	60	5.70	0.1442	0.06581	102.1
	120	5.68	0.1448	0.06232	107.1
900	15	5.84	0.1821	0.06127	96.2
	30	6.14	0.1932	0.04027	101.9
	60	6.42	0.1933	0.03971	102.7
	120	6.44	0.1929	0.03927	102.3
Cu + 5 wt. % Al$_2$O$_3$					
800	15	5.28	0.0612	0.08941	89.1
	30	5.34	0.0982	0.08827	101.2
	60	5.52	0.1191	0.08146	107.5
	120	5.58	0.1332	0.08007	109.1
900	15	5.94	0.1763	0.07413	99.1
	30	5.98	0.1824	0.06981	108.4
	60	6.14	0.1894	0.06218	118.5
	120	6.20	0.1888	0.06127	124.7

At temperatures higher than 900 °C, *e.g.*, 1000 °C, the sintered plates were distorted because of the presence of a molten phase. Due to the small size of the

Cu–Al$_2$O$_3$ nano-powders, their maximum temperature of sintering is 900 °C, which is lower than for conventional powders.[5]

The results given in Table I show that the density of the sintered samples prepared at the same sintering temperature and time decrease with increasing content of Al$_2$O$_3$. However, with increasing temperature, the density of sintered samples increases. In the higher temperature range, where the diffusion mobility of the atoms is sufficiently high, a complex diffusion mechanism of mass transport, responsible for the sintering process occurred. With increasing sintering temperature, the actions of the complex mechanisms are more intense, directly affecting the formation of contacts between the particles, contact surface growth, formation of closed pores and grain growth. Therefore, with increasing temperature, the sintered density increases with time.

The available phenomenological sintering equations are based on the kinetics description of real dispersion systems, from the analysis of relative volume change. Relative volume change represents a measure of the activity a system as a function of temperature and time and is independent of the porosity of a pressed sample.[3] Regarding this, the influence of temperature, time and different content of Al$_2$O$_3$ on the relative volume change was investigated in this study. The change of relative volume, as a measure of system activity, increased with increasing sintering temperature for the same time and Al$_2$O$_3$ content. At a given Al$_2$O$_3$ content and temperature, the relative volume change increased with increasing time of sintering. The values of the relative volume change decreased with increasing content of Al$_2$O$_3$ for a constant temperature and time of sintering. Commencing from the general kinetic equations, with the aim of analyzing the sintering kinetics, the obtained results are in accordance with other research results and certainly confirm earlier investigations on the possibility employing existing phenomenological equations of sintering.[3]

The dependence of the specific electric resistance and hardness on the temperature, time of sintering and alumina content are presented in Figs. 2 and 3, respectively.

With increasing content of Al$_2$O$_3$, the duration of the sintering process increases. However, with increasing sintering temperature for the same time, the value of specific electric resistance decreases. In accordance with all these facts and bearing in mind that the change of specific electric resistance represents a measure of the structural stabilization of the system, it can be concluded that at certain temperatures structural stabilization of the system did not occur, *i.e.*, the structural stabilization process was not completed. Also, with increased sintering temperature, the duration of the sintering process is shortened (Fig. 2). Based on the value of specific electric resistance for the system with 3 % Al$_2$O$_3$ during sintering at 800 °C, the sintering process lasted for 120 min, while for the same system sintered at 900 °C, the sintering process lasted for 30 min.

The values of hardness of the sintered samples are in agreement with the values of the specific electric resistance, *i.e.*, the structural stabilization of the sys-

tem. These results also show an increase of hardness with increasing content of Al$_2$O$_3$, for the same temperature and sintering time. The obtained hardness results are the consequence of the relatively even distribution of Al$_2$O$_3$ particles in the copper matrix. A relatively even distribution of alumina in the nano-composite system, achieved during the synthesis of the powder during deposition from the liquid phase, leads to stabilization of the dislocation structure and achievement of significant reinforcing effects by the complex action of several mechanisms. Thereby, reinforcement of the small-grain material structure can be caused by reinforcing of the grain boundaries, dissolving reinforcement and the Orowan mechanism. Also dislocations can disappear in the grain boundaries or cease to multiply, since the Frenk–Read sources of dislocations cannot be activated in small-grained multi-phase materials, which represents an additional mechanism of reinforcement.[18]
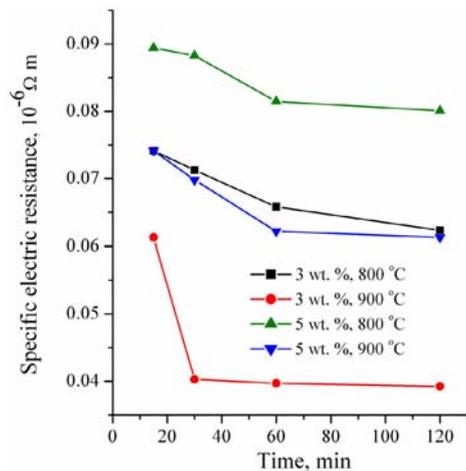
Fig. 2. Dependence of the specific electric resistance on the sintering time at different temperatures and different alumina contents.
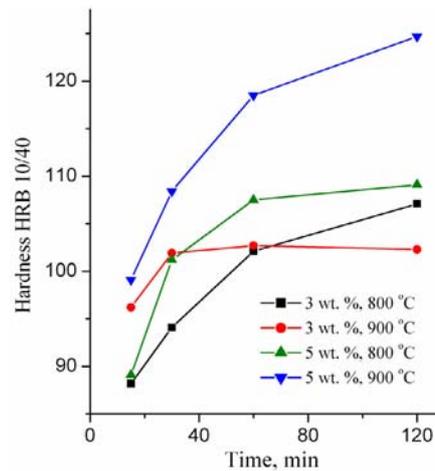
Fig. 3. Dependence of the hardness on the sintering time at different temperatures and different alumina contents.

Analysis of the electrical and mechanical properties of Cu–Al$_2$O$_3$ sintered systems showed that for the system with 3 wt. % of Al$_2$O$_3$ the structural stabilization had finished after 30 min of sintering at 900 °C, with significant reinforcement effects. For the other systems, the structural stabilization was not completed even after 120 min. As the optimal solution for the production of dispersed strengthened Cu–Al$_2$O$_3$ is the process conducted at 900 °C for 30 min with 3 wt. % of Al$_2$O$_3$, which was confirmed by microstructural analysis, presented in Figs. 4–6.

Analysis of the microstructure of the different sintered samples confirms these assumptions. The microstructure of the sample sintered at 800 °C for 30 min is given in Fig. 4, which clearly shows that the structural stabilization process was not completed. The microstructure is characterized by the formation of closed pores, typical for the medium stage of sintering. In certain areas, contacts between cer-

tain particles were achieved, which is typical for the starting stage of sintering. The microstructure of samples sintered at 900 °C for 15 and 30 min are presented in Figs. 5 and 6, respectively. The shown microstructures are characteristic for the medium (Fig. 5) and final stage (Fig. 6) of sintering, confirming the analysis of structural stabilization of the system based on the values of the specific electric resistance of sintered samples. In addition to this, a relatively even distribution of pores can be seen in the examined samples, which, together with other factors, significantly contributes to the reinforcement of the highly-conductive copper matrix.
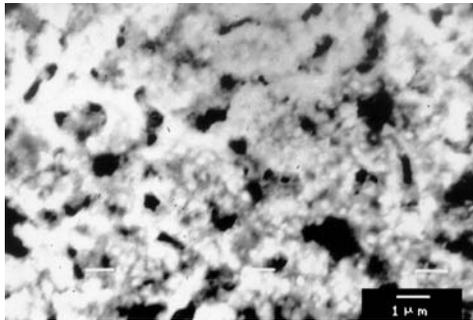
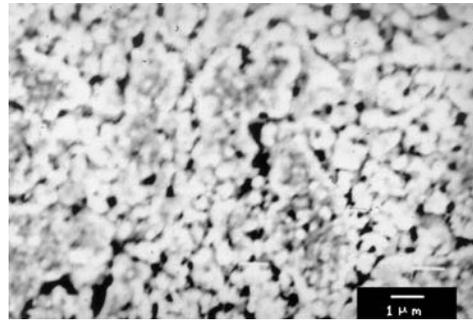Fig. 4. SEM Microphotograph of the sintered Cu + 3 wt. % Al_2O_3 system (800 °C, 30 min).

Fig. 5. SEM Microphotograph of the sintered Cu + 3 wt. % Al_2O_3 system (900 °C, 15 min).
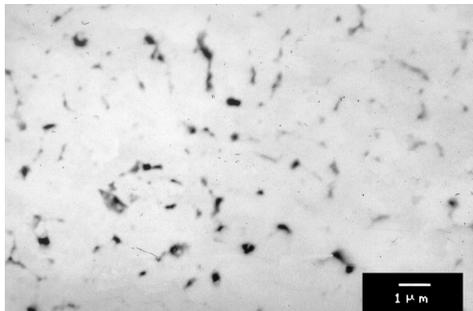

Fig. 6. SEM Microphotograph of the sintered Cu + 3 wt. % Al_2O_3 system (900 °C, 30 min).

In order to determine the distribution of elements in the structure, surface analysis of the sample was performed by EDS. The SEM microphotograph of the examined sample with the surface on which the surface scanning was performed marked is shown in Fig. 8, and the results of the examination of the sample of the sintered Cu–3 wt. % Al_2O_3 system by EDS are given in Fig. 9.

The results of surface scanning show a homogeneous distribution of elements in the structure. From Fig. 9, it can be seen that copper covers almost the entire surface of the sample. The results of surface scanning for aluminum and oxygen show that these two elements are present less in the structure of the sintered sample and the surfaces they occupy are inter-lapping, which corresponds to the existence of an Al_2O_3 dispersoid in the structure. Except for aluminum and oxygen, an inter-lapping of all three elements is also noticeable, which leads to the assumption of

the presence of a Cu$_x$Al$_y$O$_z$ phase.[10] Finally, for a detailed characterization of the third Cu$_x$Al$_y$O$_z$ phase, an apparatus of exceptionally high resolution is necessary.
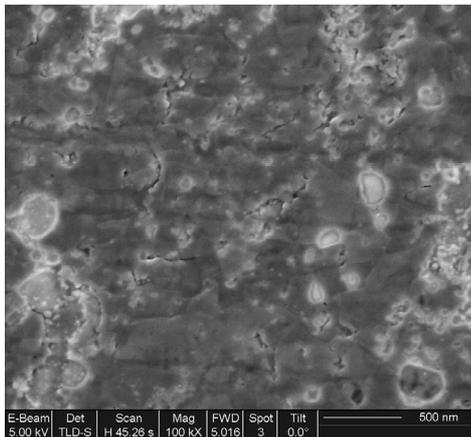

Fig. 7. Focused Ion Beam (FIB) analysis of the sintered Cu + 5 wt. % Al$_2$O$_3$ system.
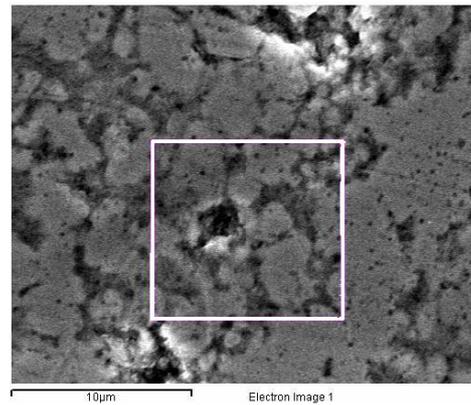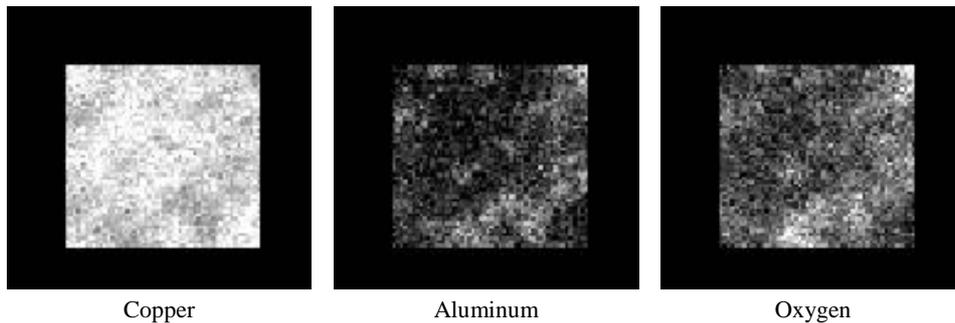

Fig. 8. SEM Microphotograph of a sintered Cu–3 wt. % Al$_2$O$_3$ sample with the surface scanning area marked.

| Copper | Aluminum | Oxygen |

Fig. 9. Surface scanning of a sintered Cu–3 wt. % Al$_2$O$_3$ sample by EDS.

CONCLUSIONS

Detailed characterization of the obtained powders indicate the possibility of the synthesis of nano-composite Cu–Al$_2$O$_3$ powders, with a particle size 20–50 nm, by a thermochemical method.

Such obtained nano-composite powders, the structures of which are preserved in the structure of the final product, enabled the production of a sintered system with exceptional reinforcement and a good combination of mechanical and electrical properties. Thus, the results of hardness examination of the sintered samples showed that the increase of the hardness is in reverse relationship to the reduction of the specific electric resistance, *i.e*., structural stabilization of the system, which was confirmed by microstructural examination. The significant effects of reinforcement achieved are the consequence of a relatively even distribution of Al$_2$O$_3$ in a copper metal matrix, already achieved in the process of pow-

der synthesis by depositing from the liquid phase. This was also confirmed by the results of analysis by EDS of the surface of the samples.

The identification of $Cu_xAl_yO_z$ phases in the structure and a study its influence on the stabilization of the dislocated structure and consequential improvement of mechanical properties, as well as the attainment of a better combination of mechanical and electrical properties of the sintered systems are essential aspects of this research, which will be continued.

ИЗВОД

СИНТЕРОВАЊЕ НАНО-КОМПОЗИТНИХ ПРАХОВА Cu–Al$_2$O$_3$
ДОБИЈЕНИХ ТЕРМОХЕМИЈСКИХ ПОСТУПКОМ

МАРИЈА КОРАЋ[1], ЗОРАН АНЂИЋ[2], МИЛОШ ТАСИЋ[2] и ЖЕЉКО КАМБЕРОВИЋ[1]

[1]*Технолошко–металуршки факултет, Карнеѓијева 4, 11000 Београд и*
[2]*Научно-истраживачки центар, Николе Пашића 26, 31000 Ужице*

У овом раду представљена је синтеза нано-композитног праха Cu–Al$_2$O$_3$ термохемијском методом и синтеровањем, уз упоредну анализу механичких и електричних својстава добијених чврстих узорака. Нано-кристални Cu–Al$_2$O$_3$ прахови добијени су термохемијском методом у следећим корацима: сушење распршивањем, оксидација полазних прахова, редукција водоником и хомогенизација. Прахови су окарактерисани аналитичком електронском микроскопијом (AEM) спрегнутом са спектроскопијом енергије расејања (EDS), диференцијалном термијском и термогравиметријском анализом (DTA–TGA) и дифракцијом X-зрака (XRD). Величина честица добијених прахова износила је 20–50 nm, уз знатно присуство агломерата. Композитни прахови карактеришу се хомогеном расподелом Al$_2$O$_3$ у бакарној матрици. Прахови су пресовани на хладно притиском од 500 MPa и синтеровани у атмосфери водоника под изотермским условима у температурном опсегу од 800 до 900 °C у трајању до 120 мин. Карактеризација Cu–Al$_2$O$_3$ синтерованог система укључивала је одређивање густине, релативне промене запремине, електричних и механичких својстава, испитивање микроструктуре техником SEM, анализом помоћу усмереног јонског снопа (FIB) и техником EDS. Добијени нано-композит, чија је структура, уз извесне промене, присутна и у коначној структури синтерованог материјала, омогућава хомогену расподелу дисперзоида у бакарној матрици синтерованог материјала, са израженим ефектима ојачања, и одличну комбинацију механичких и електричних својстава.

REFERENCES

1. J. Karch, R. Birringer, H. Gleiter, *Nature* **330** (1987) 556
2. O. Milošević, *Material Science Monograph of the Serbian Academy of Science and Arts*, *SANU*, **38** (1999) 55
3. M. M. Ristić, *Fundamental problems of material science*, Technical Faculty of Čačak and SANU, Belgrade, (2003) p. 41
4. F. H. Froes, O. N. Senkov, E. G. Baburaj, *Mat. Sci. Eng.* **A301** (2001) 44
5. Z. Anđić, M. Tasić, M. Korać, B. Jordović, A. Maričić, *Mater. Technol.* **38** (2004) 245
6. O. Vasylkiv, Y. Sakka, *J. Am. Ceram. Soc.* **84** (2001) 2489

7. Y.–Q. Wu, Y.–F. Zhang, X.–X. Huang, J.–K. Guo, *Ceram. Internat.* **27** (2001) 265
8. P. K. Jena, E. A. Brocchi, M. S. Motta, *Mater. Sci. Eng.* **A313m** (2001) 180
9. D. W. Lee, G. H. Ha, B. K. Kim, *Scripta Mater.* **44** (2001) 2137
10. P. K. Jena, E. A. Brocchi, I. G. Solórzano, M. S. Motta, *Mater. Sci. Eng.* **A317** (2004) 72
11. NanoPowder Industries, http://www.nanopowders.com/applications.htm (Jan 28, 2006)
12. M. Korać, *M.Sc. Thesis*, Faculty of Technology and Metallurgy, University of Belgrade, 2005 (in Serbian)
13. Z. Anđić, M. Korać, Ž. Kamberović, M. Tasić, *Book of Abstracts,* in *Proceeding of V Scientific Meeting: Physics and Technology of Materials, FITEM '04*, Čačak, SCG, (2004), p. 71
14. Y.–Q. Wu, Y.–F. Zhang, X.–X. Huang, J.–K. Guo, *Ceram.Internat.* **27** (2001) 265
15. P. K. Jena, E. A. Brocchi, M. S. Motta, *Mater. Sci. Eng.* **C15** (2001) 175
16. M. Entezarian, R. A. Drew, *Mater. Sci. Eng.* **A212** (1996) 206
17. D. W. Johnson Jr., D. J. Nitti, L. Berrin, *Bull. Amer. Ceram. Soc.* **51** (1972) 896
18. D. G. Morris, M. A. Morris, in *Structural Applications of Mechanical Alloying*, F. H. Froes, J. J. DeBarbadillo, Eds., ASM, Metals Park, Ohio, 1992, p. 265.